Regular Article

Aditya Rio Prabowo*, Tuswan Tuswan, Dandun Mahesa Prabowoputra and Ridwan Ridwan

Deformation of designed steel plates: An optimisation of the side hull structure using the finite element approach

https://doi.org/10.1515/eng-2021-0104
received August 14, 2021; accepted October 21, 2021

Abstract: Thin-walled structures, which generally consist of unstiffened and stiffened plates, are widely used in engineering as one of the core features of any product or construction. Due to environmental conditions and working operation, the components of the structure unavoidably become subject to various types of loading. Deformation patterns and overall behaviour are expected to be varied, as different materials are considered in the structures. In this situation, assessments are required to quantify the responses and determine the relationships between the structural behaviour and structural parameters. In this work, we attempt to obtain the behaviour data of unstiffened and stiffened plates as components of thin-walled structures. The material class – i.e. low- and medium-carbon steels – and loading parameters (i.e. type and angle) are taken as the main inputs in the finite element analysis. A geometrical design is adopted based on the side hull structure of a medium-sized tanker, for which two plate types, unstiffened and stiffened, are used. The results indicate that increasing the loading angle reduces the force experienced by the plate, while the greater the loading direction angle is, the greater the total displacement value will be. In terms of the plate design, the stiffener is observed to reduce the force expansion during the loading of the stiffened plate.

Keywords: stiffened plate, deformation pattern, material class, loading type, finite element analysis

*** Corresponding author: Aditya Rio Prabowo,** Department of Mechanical Engineering, Universitas Sebelas Maret, Surakarta, Indonesia, e-mail: aditya@ft.uns.ac.id
Tuswan Tuswan: Department of Naval Architecture, Institut Teknologi Sepuluh Nopember, Surabaya, Indonesia
Dandun Mahesa Prabowoputra: Department of Mechanical Engineering, Universitas Muhammadiyah Purwokerto, Banyumas, Indonesia
Ridwan Ridwan: Department of Mechanical Engineering, Universitas Sebelas Maret, Surakarta, Indonesia

1 Introduction

The use of thin-walled steel structures has generally increased over the last few decades, with their areas of application becoming increasingly diverse, ranging from ships to other marine platforms [1–3]. Most thin-walled designs in ship structure applications are stiffened for structural, weight conservation, and cost-effectiveness reasons. Stiffened panels are essential structural elements that form the primary structures of ships and other maritime vessels. These structures are formed of an arrangement of plates/shells reinforced with stiffeners. The reinforcement of thin-walled structures with lightweight stiffeners is a better method in most cases compared to increasing the web thickness of an unstiffened plate [4]. Stiffeners are assembled in the longitudinal or transverse direction and equally spaced over plates to ensure the strength and durability of the ship's structural components. A variety of stiffeners are usually built-in, such as flat bars (FBs), L-sections, T-profiles, I-profiles, etc.

It is crucial to conduct initial assessments of practical applications to quantify ship hulls' maximum load-carrying capacity or ultimate global strength for economic and safety reasons. Research carried out by employing analytical, numerical, and experimental approaches has revealed the influence of the structural behaviour of stiffened panels under several uncertainties, including the geometry and physical properties, applied load, and boundary conditions and constraints. Various works have analysed the ultimate strength of unstiffened or stiffened panels of ship structures under these conditions. Paik et al. [5,6] performed benchmark experiments on the ultimate limit strength measurement of unstiffened plates, stiffened panels, and ship hull girders using various approaches, including nonlinear finite element analysis (FEA) and

analytical methods. The strength measurements of stiffened [5] and unstiffened [6] panels from the bottom section of an AFRAMAX-class oil tanker under combined biaxial compression and lateral pressure have been thoroughly validated. Xu et al. [7] performed a series of computational investigations in 2013 to investigate the influence of boundary conditions and geometry on the overall strength and collapse behaviour of continuous stiffened panels of a ship's structure. A numerical investigation was also carried out by Bayatfar et al. [8] the following year. The influence of cracks on the axial compressive action between thin-walled unstiffened and stiffened plate elements indicates their significant effect on compressive strength characteristics. A novel Y-stiffener profile for ship structure was proposed in a recent paper by Leheta et al. [9]. IACS-CSR was used to measure the ultimate strength of conventional and novel Y-stiffeners for a double-hull oil tanker. Using a related scenario, Leheta et al. [10] investigated the effect of novel Y-stiffeners on the load-carrying capability of ship deck panels under a vertical hull girder bending moment numerically.

Furthermore, the ultimate and residual strengths of a hull girder based on international association of classification societies (IACS), i.e., harmonized common structure rules (CSR-H), common structure rules for oil tankers (CSR-OT), and common structure rules for bulk carriers (CSR-BC) were investigated comprehensively by Shi et al. [11]. The development of ultimate-limit state-based multiobjective optimisation was investigated by Kim and Paik [12] for application to commercial ship structural design. Moreover, according to Ma et al. [13], experimental and computational studies on the ultimate strength of stiffened plates exposed to combined biaxial compression and lateral loads revealed that the lateral pressure increased load-carrying capacity when lateral force restrained deformation. In terms of the relationship between material properties and strength assessment, a recent study conducted by Doan et al. [14] investigated the ultimate compressive strength of equivalent stiffened panels using two different materials made of aluminium and steel in a comparative numerical analysis.

As FEA has recently been adopted for assessing the structural behaviour and performance of stiffened structural parts, a series of numerical studies were carried out on stiffened panels used in different structural parts for various types of ships. The optimisation of the stiffener configuration for structural behaviour under static loading has been performed for other structural parts, including the side hull [15] and the stern ramp door [16]. Additionally, assessments of the structural behaviour of various types of ships under dynamic loads at different structural locations, such as the car deck [17] and hull [18], can be found in other studies. The effects of recent developments on the structural performance of stiffened ship structures after an impact phenomenon, such as a ship–ship collision accident, ship grounding, or other forms of ship hull damage, and the structural crashworthiness need to be reviewed in detail in more advanced analyses. An assessment of the effect of a series of grounding scenarios on crashworthiness in an oil/chemical thin-walled double-bottom tanker was investigated by Prabowo et al. [19]. To determine the ultimate limit and potential damage that has occurred during the event, a failure criterion was introduced. Using the same ship data, a further simulation of the impact of a ship hull under grounding with a conical rock on its operation is described in detail in ref. [20]. In this work, nonlinear FEA was used to simulate the influence of mesh size parameters on the structural response and contours of the ship hull under impact loading.

Moreover, besides grounding incidents, descriptions of ship–ship collision accidents under different scenarios can be found in the literature. In 2016, Bae et al. [21] performed numerical simulations using nonlinear analysis to investigate the virtual experimental data for several collision scenarios based on actual accident cases. Element formulations, friction coefficients, and material models were used as the number of parameters in the integrated study. The rebounding phenomena of a striking RoRo ship and its impact on the crashworthiness of the struck ship were thoroughly studied the following year by Prabowo et al. [22]. For all full-scale proposed collision scenarios, it was discovered that there is a strong equivalence between internal energy and crushing force. More advanced analyses of stiffened ship structures subjected to impact phenomena were performed in a series of recent studies to identify structural damage caused by maritime accidents, including ship–ship collision accidents [23,24], ship grounding [25], and other forms of ship hull damage [26,27].

According to the above-mentioned literature articles and the core design used in the ship building industry, reviews of the research work on the deformation pattern and structural behaviour of stiffened and unstiffened plates used in ship structures under comprehensive parameters are limited. There have been a few studies on the structural evaluation of stiffened panels subjected to a centralised load, particularly in cases where the side hull collides with something with a sharp tip. However, it is necessary to investigate the possibility that a ship structure will be damaged by a variety of accidents, including collisions and stranding with other objects. In fact, the force experienced during stranding has an uncertain direction, resulting in an uncertain force distribution across the stiffened hull plate.

A systematic numerical-based study on deformation assessment between stiffened plates using a FB and

unstiffened plates under a material class and loading parameters was conducted to address these issues. The present study aims to further investigate the influence of variations in the material type, stiffener, type of loading, and angle of loading on the von Mises stress, total displacement, and equivalent strain value using FEA. In this regard, the geometry and cross-section of the side hull structure of a medium-sized tanker are used as references for modelling using the Ansys Workbench.

2 Finite element modelling strategy

2.1 Candidate model and mechanical properties

The current investigation considered two structural components, unstiffened and stiffened thin-walled plates, for the current benchmark study. The extent and geometrical dimensions of these reference models are based on previous studies published in ref. [28]. For modelling purposes, in the first step, the geometry of the thin-walled plates is created using Autodesk Fusion 360 software. The illustration of the 2D thin-walled plate cross-section is shown in Figure 1. The thin-plate length and width are 1,200 and 720 mm, respectively. The plate's thickness is 5 mm. Two types of plates are used in the simulation, the unstiffened plate and the plate using a FB stiffener, as presented in Figure 2. The FB stiffeners are described by their height and thickness, which are 120 and 6 mm, respectively.

In this simulation, two material variations are used: low-carbon steel material with steel AISI 1006 85 HR and medium-carbon steel with the steel AISI 1045 HR HV specifications. A homogeneous material isotropic with elastic properties is assumed in this FEA. The physical properties of the two proposed materials are shown in Table 1.

2.2 Consideration of variation model scenario

In this section, the model scenario is based on a combination of the material type, stiffener use, type of loading, and direction of the loading angle. A total of eight main

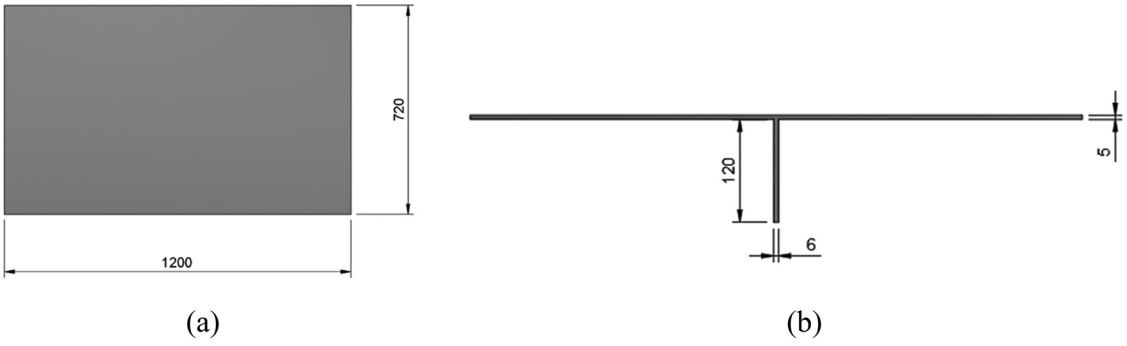

Figure 1: Illustration of a 2D thin-walled plate cross-section: (a) top-view plate cross-section and (b) side-view plate cross-section.

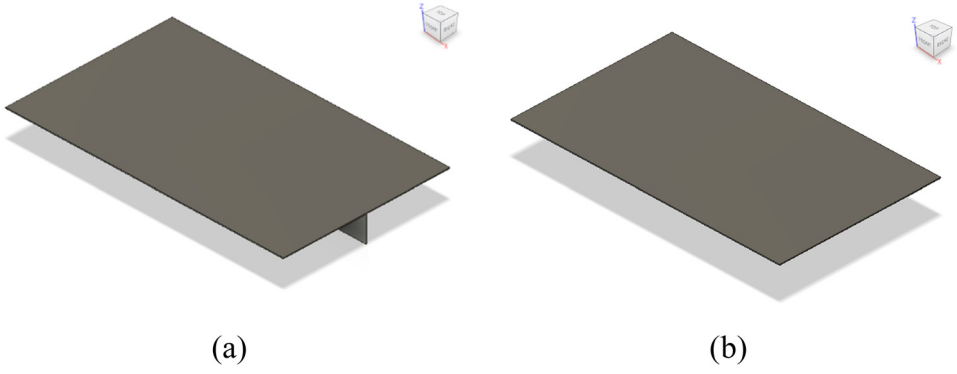

Figure 2: Three-dimensional plate design configurations: (a) stiffened plate using a FB and (b) unstiffened plate.

Table 1: Material physical properties for AISI 1006 and AISI 1045

Material properties	AISI 1006	AISI 1045
Density	7.872×10^{-6} kg/mm^3	7.87×10^{-6} kg/mm^3
Modulus elasticity	200,000 MPa	200,000 MPa
Poisson's ratio	0.29	0.29
Yield strength	285 MPa	450 MPa
Ultimate tensile strength	330 MPa	585 MPa

variations are analysed, starting with variations in the material type, FB stiffener utilisation, and type of loading. Further, from each of the variations, the simulations are then extended by investigating the influence of loading angles. In this work, the loading angle was varied in the direction of the positive *Y*-axis, namely, 0, 15, 30, 45, 60, and 75°. Furthermore, a total of 8 main variations with 48 simulations were comprehensively compared. Figure 3 illustrates the diagram of the simulation variation scenario.

2.3 Finite element model discretisation

In this project, Autodesk Fusion 360 was used as the FEA platform for the modelling and simulation phases. The procedure used for FE simulation can be divided into three steps: (1) pre-processing was carried out, which involves modelling the geometry of the structures, meshing, and assembling the mass and stiffness matrices. The 3D conceptual modelling of stiffened and unstiffened structures was optimized using Autodesk Fusion 360; (2) finite analysis was performed in 48 simulation models using a static structural method to obtain structural responses; and (3) post-processing was used to evaluate the desired response output.

In the model discretisation, the stiffened plate was modelled using solid elements. Salomon [29] investigated topics similar to those covered in this paper and developed an analytical theory for describing various deflection phenomena in a shell model and 3D model (solid). The results demonstrated that the thickness of the modelled stiffener has a significant effect on the displacement solution. Before the principal analysis, a convergence assessment was carried out to find the appropriate mesh size for specific geometries with solid elements. In this work, element length-to-thickness ratios in the range of 5–10 were used to investigate structural responses – i.e., stress, displacement, and strain – to determine the most appropriate mesh size. In the FE setting, the mesh sizes were set to range from 10 to 70 mm. The results of the analysis indicated that the mesh size tends to be stable in the range of 20–50 mm, as can be seen in Figure 4.

In this regard, fixed constraints ($U_x = U_y = U_z = 0$) were adopted on four sides of the plate. The plate was then given a static loading force with a magnitude of 5,000 N vertically (*Y*-axis) on the upper side of the plate, with the assumption there is no force in the other direction (*X*- and *Z*-axis). The load was carried out perpendicular to the upper section of the plate using two different

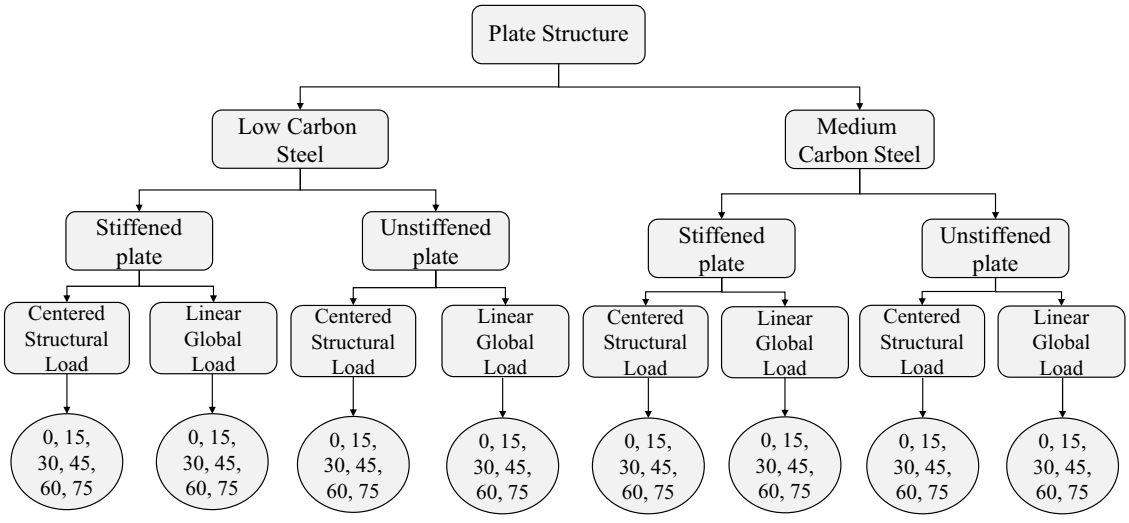

Figure 3: Diagram of the simulation variation scenario.

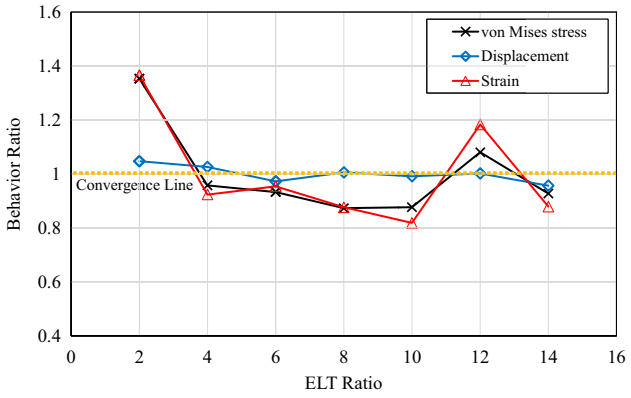

Figure 4: Summary of the convergence assessment of the plate with one longitudinal stiffener.

scenarios – centred structural load and global linear load – as shown in Figure 5.

3 Discussion of numerical results

3.1 Validation test

The responses to the FEA and experimental tests were compared for validation purposes considering the von Mises stress, displacement, and strain of the plates with one longitudinal stiffener (FB). In previous research [28], the authors performed a series of panel penetration tests with a cone-shaped indenter at the centre of the plate on a plate with one longitudinal stiffener. The geometrical configuration and set-up we used referred to the experimental test in this numerical analysis [28]. The validation test was conducted by analysing the penetration experimental result, as illustrated by force–indentation curves at a load 5,000 N. Table 2 shows the comparison of von Mises stress, displacement, and strain between the

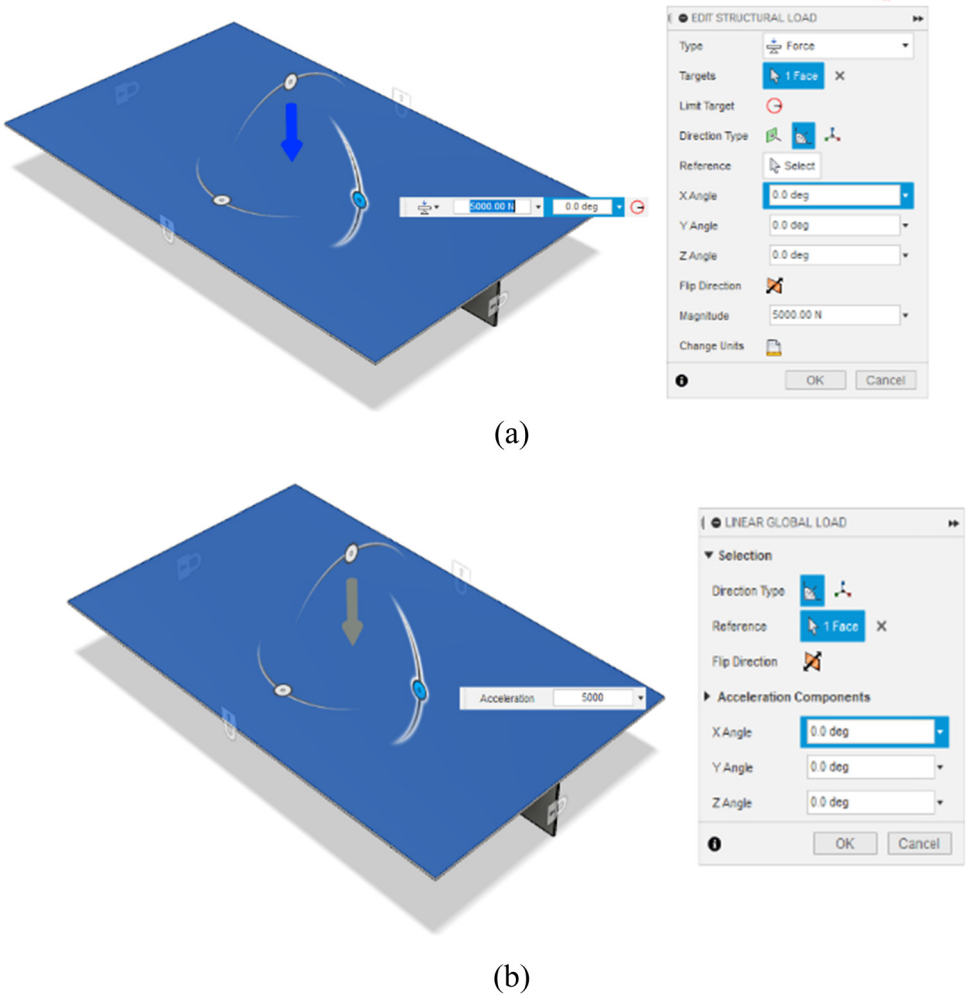

Figure 5: Loading conditions on the finite element geometry: (a) centred structural load and (b) global linear load.

Table 2: Validation test carried out for an FEA and experimental test

Plate with one longitudinal stiffener	FEA (present study)	Experimental test [28]	Error (%)
Von Mises stress	28.66	26.56	7.9
Displacement	0.121	0.135	10.4
Strain	0.00014	0.00013	7.7

present study and the previous test for a plate with one longitudinal stiffener subjected to a centred structural load. The mean error of the numerical result at 8.7% indicates the good agreement of the proposed finite element modelling.

3.2 Comparison result of von Mises stress

The strength assessment of ship plates is necessary in order to quantify the deformation and stress states and determine the relationships between the structural behaviour and structural parameters. The observations of von Mises stress show the von Mises stress between stiffened and unstiffened plates for all evaluated parameters. Here, it is also necessary to analyse whether the von Mises stress experienced by the plate exceeds the yield strength of the material or not. Figure 6 compares von Mises stress using stiffened and unstiffened low-carbon steel materials for different loading types and angles. These results show that both the stiffened and unstiffened plates experience stress reduction along with an increasing loading angle when subjected to a centred structural load or linear global load. It can be found that the highest stress value, which is 1,248 MPa, occurs in an unstiffened plate subjected to a global linear load at an angle of 0°. Meanwhile, the smallest stress value, which is 8.007 MPa, is experienced on a stiffened plate subjected to a centred structural load at the load angle of 75°. Further, the yield strength value of low carbon steel is assumed to be 285 MPa. Therefore, with a 5,000 N loading force, stiffened and unstiffened plates subjected to a global linear load enter a failure condition, because they have a value that exceeds the yield strength. However, the von Mises value of the plates subjected to centred structural load is still below the yield strength, as depicted in Figure 6.

Next, Figure 7 presents the simulation result of the von Mises of stiffened and unstiffened medium-carbon steel material for different loading types and angles. The results show a similar phenomenon as the behaviour seen in the low-carbon material. In the stiffened and unstiffened plates subjected to both loading conditions, the von Mises stress decreases along with the increasing loading angle. It can be found that the highest stress value occurs in the unstiffened plate with a global linear load at an angle of 0°, for which the magnitude is about 1,244 MPa. Meanwhile, the smallest stress with a magnitude of 7.99 MPa occurs on a stiffened plate subjected to a centred structural load at an angle of 75°. It is known from the material data that the yield strength of the medium-carbon steel is 450 MPa. The stiffened and unstiffened plates subjected to global linear loads with a magnitude at 5,000 N experience a failure condition because the value exceeds the yield strength, except for the loading angle of 75° for both stiffened and unstiffened plates. However, the von Mises value of both plates subjected to centred structural loads is far below the yield strength in all evaluated loading angles.

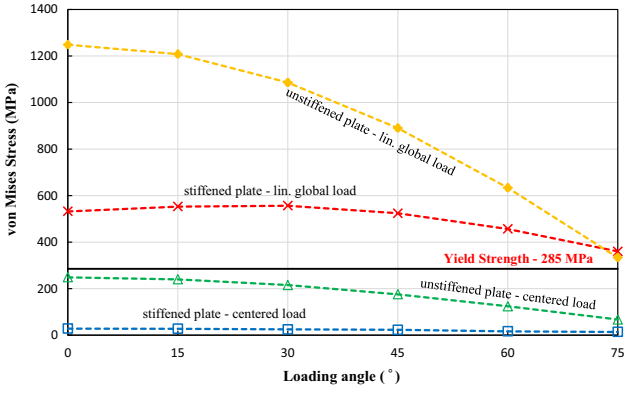

Figure 6: Maximum von Mises stress of stiffened and unstiffened low-carbon steel materials.

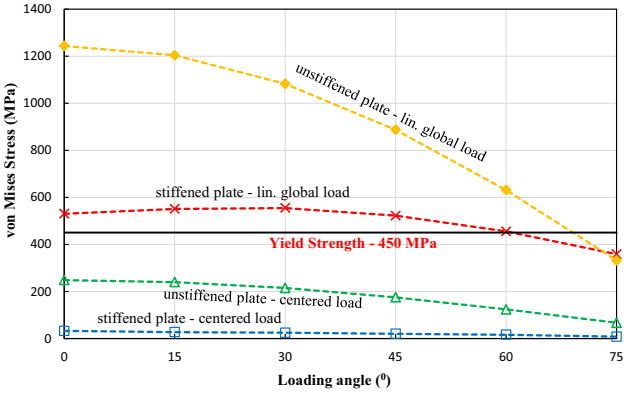

Figure 7: Maximum von Mises stress of stiffened and unstiffened medium-carbon steel materials.

3.3 Comparison result of the displacement value

This section uses a displacement value to determine displacement distribution experienced by plates due to the applied load. Figure 8 illustrates the total displacement calculated from the simulation of stiffened and unstiffened low-carbon steel plates. These results show that the displacement of both plates with two different applied loads decreases along with the increase in the direction of the loading angle. As seen in Figure 8, the highest displacement occurs on an unstiffened plate with a global linear load at an angle of 0° with a magnitude of 47.82 mm. In contrast, the stiffened plate with a centred load at an angle of 75° has the smallest displacement, with a magnitude of 0.04165 mm. Furthermore, the displacement data for stiffened and unstiffened medium-carbon steel plates are illustrated in Figure 9. The same phenomenon can be found compared to the displacement data shown in Figure 8. As can be seen, the displacement value decreases with the increase in the loading angle direction for all evaluated models. It can be found that the most significant displacement, with a value of 47.69 mm, occurs on an unstiffened plate with a global linear load with an angle of 0°, while the most minor displacement occurs on the stiffened plate subjected to a centred structural load with an angle of 75°.

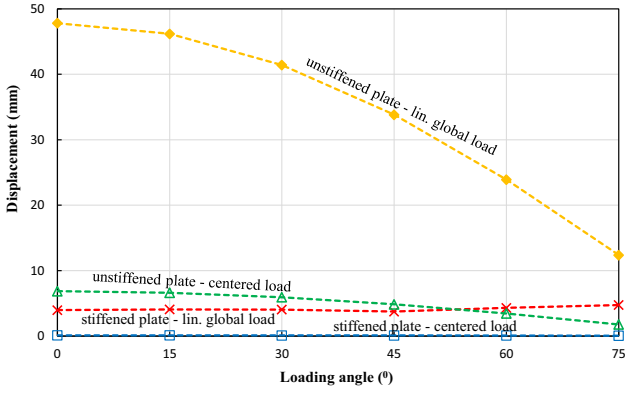

Figure 8: Maximum displacement value of stiffened and unstiffened low-carbon steel materials.

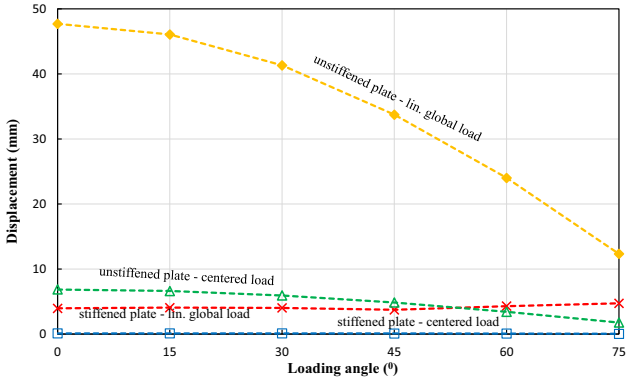

Figure 9: Maximum displacement value of stiffened and unstiffened medium-carbon steel materials.

3.4 Comparison result of the equivalent strain

Equivalent strain is a scalar quantity used to describe the state of the obtained strain. Figure 10 shows the equivalent strain data from the finite element result of both stiffened and unstiffened low-carbon steel plates. From these results, it can be seen that the equivalent strain decreases along with the increasing load angle for both types of materials. The largest equivalent strain, with a magnitude of 0.00557, can be found in an unstiffened plate with a global linear loading at an angle of 0°, while the smallest equivalent strain can be seen in a stiffened plate with a centred structural load at an angle of 75°. Further, the equivalent data for medium-carbon steel plates are illustrated in Figure 11. A similar phenomenon can be found in the equivalent data for low-carbon steel plates, where the largest equivalent strain occurs on an unstiffened plate with a global linear load at an angle of 0°. In contrast, the smallest value can be found in the stiffened plate with a centred structural load at an angle of 75°.

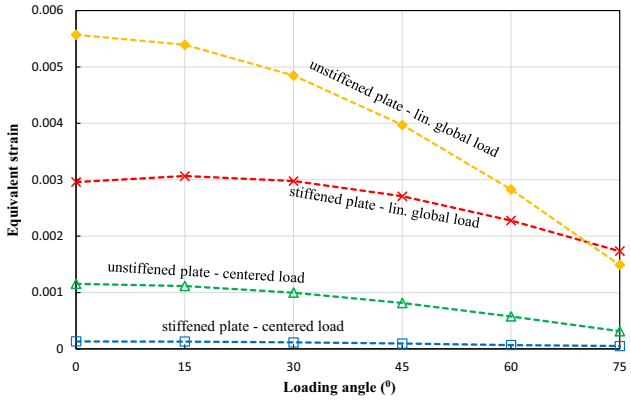

Figure 10: The equivalent strain of stiffened and unstiffened low-carbon steel materials.

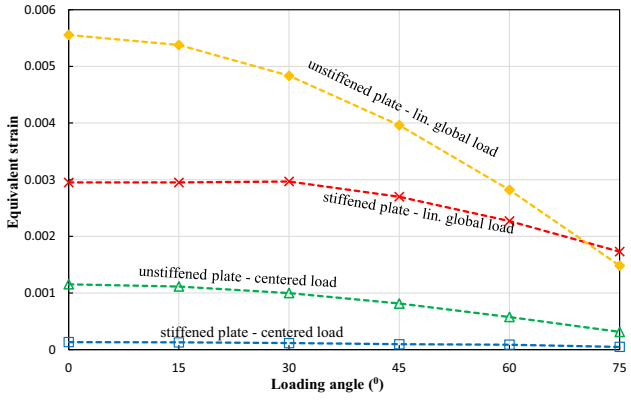

Figure 11: The equivalent strain of stiffened and unstiffened medium-carbon steel materials.

3.5 Overall discussion

As can be summarised from the analysis result, it was discovered that each variation and all the simulation parameters were unique. First, the material type parameter showing the difference between the low- and medium-carbon steel, as shown in Figures 6–11, reveals that the stress, displacement, and equivalent strain values recorded in low-carbon steel materials do not differ much from those found in medium-carbon steel. This may be because the plate has a similar geometry and cross-section. However, the maximum von Mises stress obtained from all models shows that low- and medium-carbon steels can be considered to fail when subjected to a force load of 5,000 N. In the FEA carried out using the low-carbon steel material, the highest stress occurs in an unstiffened plate with a global linear load at an angle of 0° and is equal to 1,248 MPa, whereas the yield strength of the low-carbon steel is only 285 MPa. Meanwhile, for medium-carbon steel material, the highest stress value recorded in the unstiffened load subjected to a centred structural load plate at an angle of 0° is 1,244 MPa, whereas the yield strength of this material is only 450 MPa. The other combination of variations was found using a simulation of variations with a stiffener. In the simulation, one flat plate is reinforced using a stiffener along the length of the plate. The shape and dimensions of the stiffener are presented in Figures 1 and 2, while the others are not given any reinforcement. In this variation, the plates that do not use a stiffener (unstiffened plate) have higher stress and displacement values than the stiffened plate, as reported in Figures 12 and 13. For the purpose of comparing the contour of the simulation results, Table 3 contains detailed information on eight main variation models.

Figure 12 presents the contour of von Mises stress at a loading angle of 0° between stiffened and unstiffened plates. The maximum value recorded for von Mises stress in Model 2 (using stiffener) is 532 MPa, the maximum

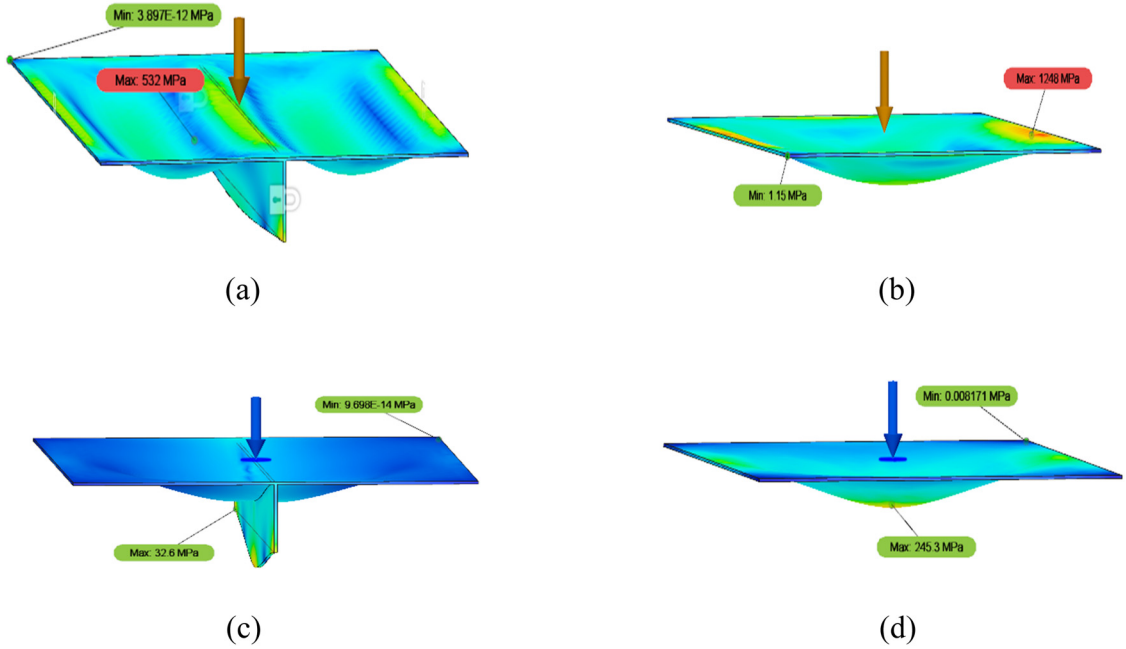

Figure 12: The contour of the von Mises stress simulation results between stiffened and unstiffened plates at a load angle of 0° for low-carbon steel with a global linear load (Models 2 and 4) and medium-carbon steel with a centred structural load (Models 5 and 7): (a) Model 2, (b) Model 4, (c) Model 5, and (d) Model 7.

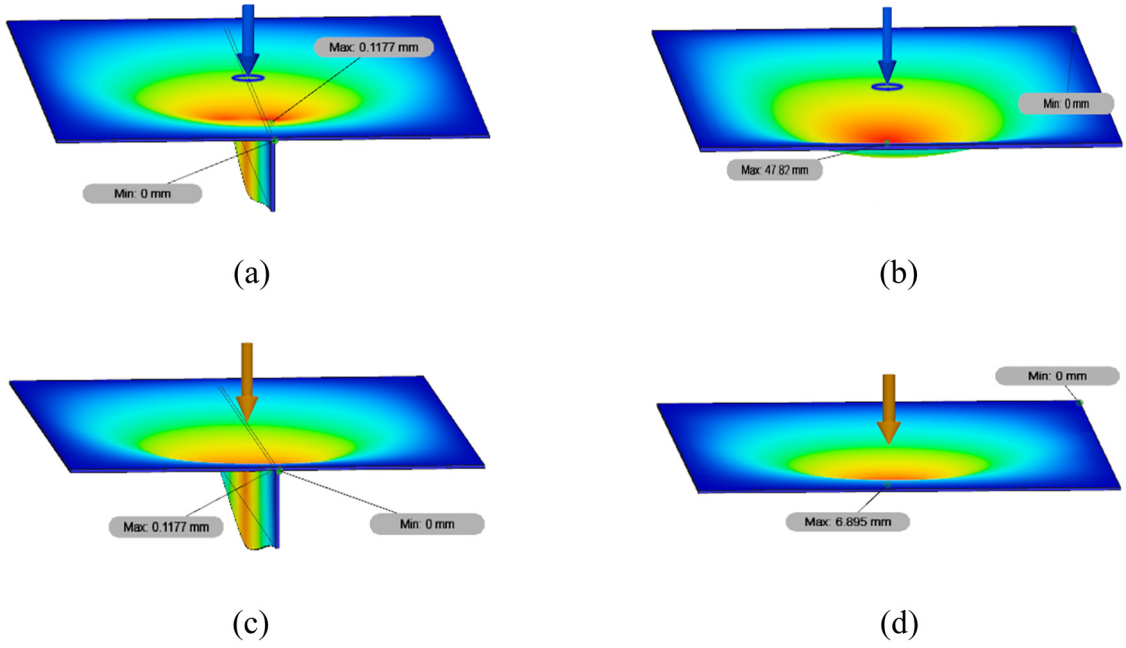

Figure 13: The contour of displacement at a load angle of 0° between stiffened and unstiffened low-carbon steel with a centred load (Models 1 and 3) and medium-carbon steel with a global linear load (Models 6 and 8): (a) Model 1, (b) Model 3, (c) Model 6, and (d) Model 8.

Table 3: Eight main variation models

Model	Variation details
1	Stiffened low-carbon steel plate with a centred structural load
2	Stiffened low-carbon steel plate with a global linear load
3	Unstiffened low-carbon steel plate with a centred structural load
4	Unstiffened low-carbon steel plate with a global linear load
5	Stiffened medium-carbon steel plate with a centred structural load
6	Stiffened medium-carbon steel plate with a global linear load
7	Unstiffened medium-carbon steel plate with a centred structural load
8	Unstiffened medium-carbon steel plate with a global linear load

stress recorded for Model 4 (without stiffener) is 1,248 MP, the maximum stress recorded for Model 5 (using stiffener) is 32.6 MPa, and the maximum stress recorded for Model 7 (without stiffener) is 245.3 MPa. The data shown in Figure 12 demonstrate that the application of a stiffener can reduce the stress received by the plate, meaning that the plate becomes stronger.

Figure 13 displays the maximum displacement at a loading angle of 0°. The maximum total displacement of Model 1 (using stiffener) subjected to a centred structural load is 0.1177 mm, while that of Model 3 (without stiffener) is 47.82 mm. Moreover, in Model 6 (using stiffener) subjected to global linear load, the maximum total displacement value is 0.1177 mm, and that in Model 8 (without stiffener) is 0.6895 mm. The data provided in Figure 13 show that the application of a stiffener can reduce the displacement received by the plate, meaning that the plate becomes stronger.

In addition, it is important to take into account the uniqueness of the strain values for FB stiffener applications. Unstiffened plates tend to have a higher equivalent strain than plates that use a stiffener. In all simulations using plates with a stiffener, the minimum strain results are 0, while in plate simulations for plates without a stiffener, the results are less than 0, which varies according to the direction of the loading angle. This shows that the stiffener can reduce the force distribution received by the plate. All these facts can be seen in Figures 10 and 11.

Next, comparing the result gained between the two types of loadings, it can be seen that the centred

structural and global linear loads have different characteristics. In global linear loads, the force is distributed over the surface of the plate, while in centred structural loads the force is concentrated at one point in the middle of the upper surface of the plate. In the variations of this type of loading, there is some uniqueness in that the stress, displacement, and strain values for the centred structural load are smaller than those for the global linear load. This is caused by the fact that the cross-sectional area of the plate subjected to a force in the simulation with a centred structural load is smaller than that subjected to a global linear load. The stress and displacement values are shown in Figures 14 and 15, and the strain values can also be seen in Figures 10 and 11.

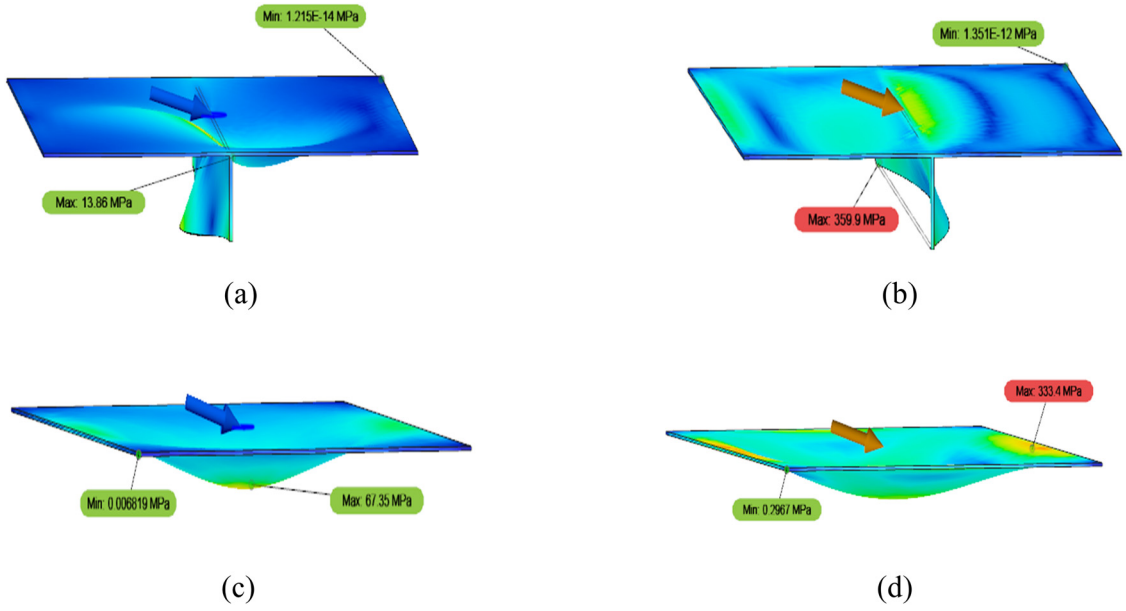

Figure 14: The von Mises stress contour at a load angle of 75° between stiffened and unstiffened low-carbon steel plates with a centred load (Models 1 and 3) and global linear load (Models 2 and 4): (a) Model 1, (b) Model 2, (c) Model 3, and (d) Model 4.

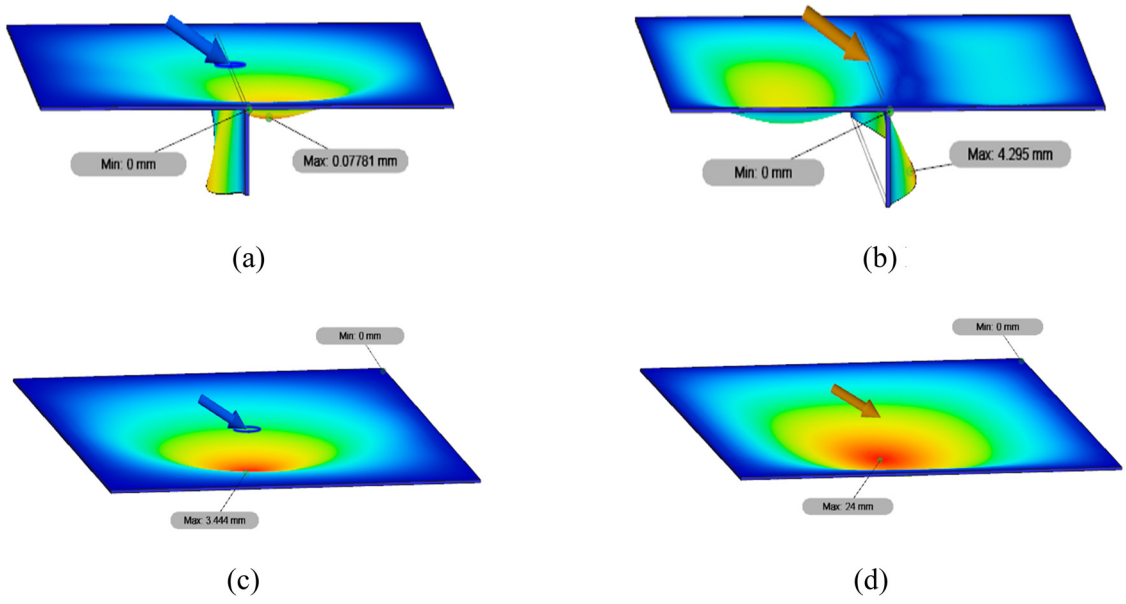

Figure 15: The displacement contour at a load angle of 60° between stiffened and unstiffened low-carbon steel plates with a centred load (Models 5 and 7) and a global linear load (Models 6 and 8): (a) Model 5, (b) Model 6, (c) Model 7, and (d) Model 8.

Figure 14 presents the maximum von Mises stress at a load angle of 75° between stiffened and unstiffened low-carbon steel plates with centred loads and global linear loads. It can be seen that the maximum value of von Mises stress recorded for Model 1 (centred structural load) is 13.86 MPa, while in Model 2 (global linear load) it is 359.9 MPa. In Model 3 (centred structural load), the maximum von Mises stress is 63.75 MPa, and in Model 4 (global linear load) it is 333.4 MPa. This indicates that the stress on the central point load is smaller than the distributed load.

Figure 15 shows the maximum displacement at a load angle of 60° between stiffened and unstiffened low-carbon steel plates with centred and global linear loads. It can be seen that the maximum total displacement in Model 5 (centred structural load) is 0.07781 mm while that in Model 6 (global linear load) is 4.295 mm. Meanwhile, in Model 7 (centred structural load), the maximum total displacement value is 3.444 mm, and in Model 8 (global linear load), it is 24 mm. The results indicate that the displacement value in the centred structural load is smaller than the global linear load in all other types of loading variations.

In the final part, the influence of the use of loading angles of 0, 15, 30, 45, 60, and 75° is evaluated. The uniqueness of the simulation results with this variation is that almost all types of variations show the trend that the greater the angle of the load, the smaller the values of maximum and minimum stress, displacement, and strain. This can occur because the greater the loading direction angle, the less optimal load force is distributed across the plate. The comparison of stress and displacement values with the variation in loading angles is shown in Figures 16 and 17, and the strain values can be seen in Figures 10 and 11.

In Figure 16, the maximum values of von Mises stress in Model 2 with loading angles of 0, 30, and 75° are shown. The maximum value of von Mises stress at an angle 0° is 532 MPa; at 30°, the maximum is 556.6 MPa and at 75° the maximum is 359.9 MPa. Figure 17 shows the maximum values of the total displacement of Model 7 with loading angles of 0, 30, and 75°. As can be seen, the maximum total displacement value at an angle of 0° is 6,895 mm; at 30°, the maximum is 5,969 mm and at 75° the maximum is 1,781 mm. These data indicate that the greater the loading direction angle, the smaller the maximum stress value.

Furthermore, there is a peculiarity in the stiffened plate with a global linear load for both low- and medium-carbon steel materials. The greater the angle of loading, the greater the total displacement obtained. This may be due to the force on the global linear load across the

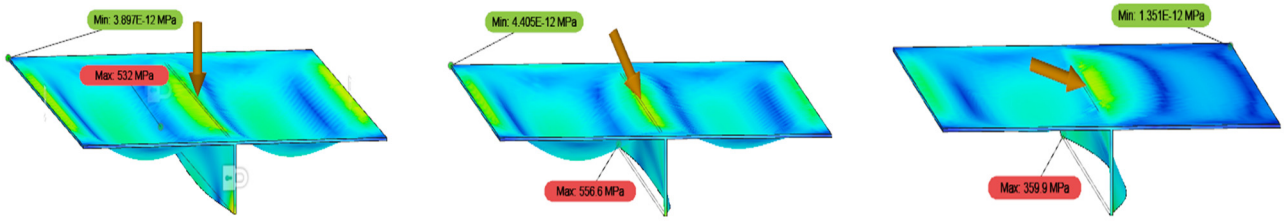

Figure 16: The contour of the von Mises stress of stiffened low-carbon steel material subjected to a linear global load (Model 2) at the loading angles of (a) 0°, (b) 30°, and (c) 75°.

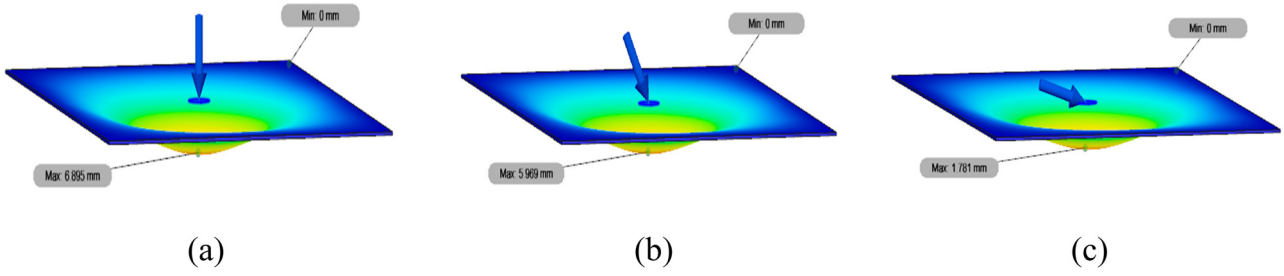

Figure 17: The displacement contour of unstiffened medium-carbon steel plates subjected to a centred structural load (Model 7) at the loading angles of (a) 0°, (b) 30°, and (c) 75°.

surface of the plate when the applied loading force direction varies. The stiffener function in the middle of the plate as well as that perpendicular also seems less effective in withstanding the force load across the entire surface of the plate. As the loading direction is in the same direction as the positive *Y*-axis, the force will be more distributed across the plate side on the positive *Y*-axis, while on the plate side on the negative *Y*-axis the force load will be held back by the stiffener. Therefore, the greater the angle of the loading direction, the greater the force on the side of the plate on the positive *Y*-axis, meaning that a greater total displacement is obtained, as shown in Figure 18. The maximum displacement shown in Model 2 at an angle of 15° is 4.069 mm, while the maximum in Model 2 at an angle of 45° is 3.737 mm. In Model 6 at an angle of 15°, the maximum displacement is 4.058 mm, while that in Model 6 at an angle of 45° is 3.727 mm. The data given in Figure 18 show that the greater the loading angle, the higher the total displacement occurring in the plate.

4 Summary and concluding remarks

In this article, the influence of variations in the material type, stiffener, type of loading, and angle of loading on the von Mises stress, total displacement, and equivalent strain value was investigated using FEA. Based on the material applications, low- and medium-carbon steels were found to be unable to withstand a force load of 5,000 N, as seen from the maximum value of stress measured being greater than the yield strength value. In the next analysis, the stiffener application was considered to be adequate for strengthening the plate. It was shown through the simulation results that the plates for which no stiffener was used had greater stress, displacement, and strain values than the plates for which no stiffener was used. The stiffener can reduce the force distribution received by the plate. In all simulation variations in which stiffener was used, the minimum strain value was 0, while in the plate simulation for which no stiffener was used, the results were less than 0.

The values recorded for stress, displacement, and strain for plates with a centred structural load were smaller than those recorded for plates with a global linear load. This is due to the fact that in simulations with a centred structural load, the cross-sectional area of the plate subjected to the force is smaller than the cross-sectional area of the plate subjected to the force with a global linear load. By increasing the loading angle, the force received by the plate will be reduced because the force tends to point to the side of the plate rather than being fully distributed across the plate. Finally, in each simulation with global linear load and stiffener variations, the greater the angle of the loading direction, the greater the

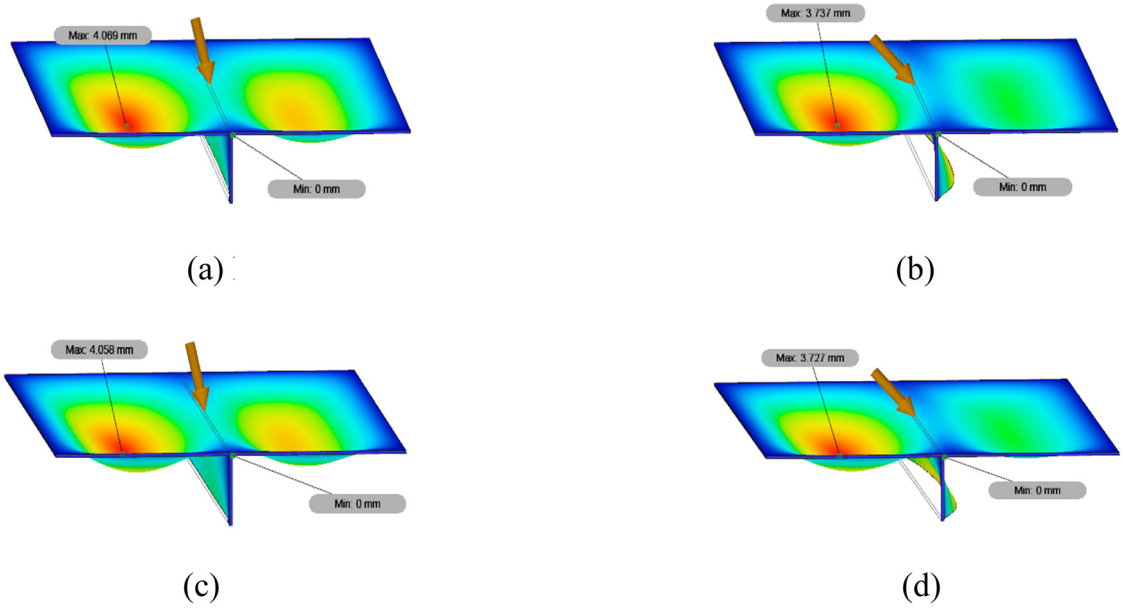

Figure 18: The displacement contour of stiffened low-carbon steel plate with a global linear load (Model 2) at an angle of (a) 15° or (b) 45° and stiffened medium-carbon steel plate with a global linear load (Model 6) at an angle of (c) 15° or (d) 45°.

total displacement value. This is caused by the force load on plates with a global linear load being distributed fully across the entire surface of the plate, meaning that the stiffener function in the middle of the plate seems less effective in withstanding the force load applied across the whole surface of the plate.

Author contributions: All authors have accepted responsibility for the entire content of this manuscript and approved its submission.

Conflict of interest: The authors state no conflict of interest.

Data availability statement: The authors declare that all data supporting the findings of this study are available within the article.

References

[1] Zubaydi A, Haddara MR, Swamidas ASJ. Damage identification in a ship's structure using neural networks. Ocean Eng. 2002;29(10):1187–200. doi: 10.1016/S0029-8018(01)00077-4.

[2] Prabowo AR, Tuswan T, Ridwan R. Advanced development of sensors' roles in maritime-based industry and research: from field monitoring to high-risk phenomenon measurement. Appl Sci. 2021;11(9):3954. doi: 10.3390/app11093954.

[3] Jen CY, Tai YS. Deformation behavior of a stiffened panel subjected to underwater shock loading using the nonlinear finite element method. Mater Des. 2010;31(1):325–35. doi: 10.1016/j.matdes.2009.06.011.

[4] Kumar PR, Gupta G, Shamili GK, Anitha D. Linear buckling analysis and comparative study of un-stiffened and stiffened composite plate. Mater Today: Proc. 2018;5(2):6059–71. doi: 10.1016/j.matpr.2017.12.211.

[5] Paik JK, Kim BJ, Seo JK. Methods for ultimate limit state assessment of ships and ship-shaped offshore structures: part I-Unstiffened plates. Ocean Eng. 2008;35(2):261–70. doi: 10.1016/j.oceaneng.2007.08.004.

[6] Paik JK, Kim BJ, Seo JK. Methods for ultimate limit state assessment of ships and ship-shaped offshore structures: part II stiffened panels. Ocean Eng. 2008;35(2):271–80. doi: 10.1016/j.oceaneng.2007.08.007.

[7] Xu MC, Yanagihara D, Fujikubo M, Guedes Soares C. Influence of boundary conditions on the collapse behaviour of stiffened panels under combined loads. Mar Struct. 2013;34:205–25. doi: 10.1016/j.marstruc.2013.09.002.

[8] Bayatfar A, Khedmati MR, Rigo P. Residual ultimate strength of cracked steel unstiffened and stiffened plates under longitudinal compression. Thin-Walled Struct. 2014;84:378–92. doi: 10.1016/j.tws.2014.07.002.

[9] Leheta HW, Badran SF, Elhanafi AS. Ship structural integrity using new stiffened plates. Thin-Walled Struct. 2015;94:545–61. doi: 10.1016/j.tws.2015.05.018.

[10] Leheta HW, Elhanafi AS, Badran SF. A numerical study of the ultimate strength of Y-deck panels under longitudinal in-plane compression. Thin-Walled Struct. 2016;100:134–46. doi: 10.1016/j.tws.2015.12.013.

[11] Shi G-J, Gao D-W, Zhou H. Analysis of hull girder ultimate strength and residual strength based on IACS CSR-H. Math Probl Eng. 2019;2019:2098492. doi: 10.1155/2019/2098492.

[12] Kim DH, Paik JK. Ultimate limit state-based multi-objective optimum design technology for hull structural scantlings of merchant cargo ships. Ocean Eng. 2017;129:318–34. doi: 10.1016/j.oceaneng.2016.11.033.

[13] Ma H, Xiong Q, Wang D. Experimental and numerical study on the ultimate strength of stiffened plates subjected to combined biaxial compression and lateral loads. Ocean Eng. 2021;228:108928. doi: 10.1016/j.oceaneng.2021.108928.

[14] Doan VT, Liu B, Garbatov Y, Wu W, Guedes Soares C. Strength assessment of aluminium and steel stiffened panels with openings on longitudinal girders. Ocean Eng. 2020;200:107047. doi: 10.1016/j.oceaneng.2020.107047.

[15] Tuswan T, Abdullah K, Zubaydi A, Budipriyanto A. Finite-element analysis for structural strength assessment of marine sandwich material on ship side-shell structure. Mater Today Proc. 2019;13(1):109–11. doi: 10.1016/j.matpr.2019.03.197.

[16] Tuswan T, Zubaydi A, Piscesa B, Ismail A, Ariesta RC, Ilham MF, et al. Influence of application of sandwich panel on static and dynamic behaviour of ferry ro-ro ramp door. J Appl Eng Sci. 2021;19(1):208–16. doi: 10.5937/jaes0-27708.

[17] Tuswan T, Zubaydi A, Piscesa B, Ismail A. Dynamic characteristic of partially debonded sandwich of ferry ro-ro's car deck: a numerical modelling. Open Eng. 2020;10:424–33. doi: 10.1515/eng-2020-0051.

[18] Ismail A, Zubaydi A, Piscesa B, Ariesta RC, Tuswan T. Vibration-based damage identification for ship sandwich plate using finite element method. Open Eng. 2020;10(1):744–52. doi: 10.1515/eng-2020-0086.

[19] Prabowo AR, Cahyono SI, Sohn JM. Crashworthiness assessment of thin-walled double bottom tanker: a variety of ship grounding incidents. Theor Appl Mech Lett. 2019;9(5):320–7. doi: 10.1016/j.taml.2019.05.002.

[20] Prabowo AR, Putranto T, Sohn JM. Simulation of the behavior of a ship hull under grounding: effect of applied element size on structural crashworthiness. J Mar Sci Eng. 2019;7:270. doi: 10.3390/jmse7080270.

[21] Bae DM, Prabowo AR, Cao B, Zakki AF, Haryadi GD. Study on collision between two ships using selected parameters in collision simulation. J Mar Sci Application. 2016;15(1):63–72. doi: 10.1007/s11804-016-1341-2.

[22] Prabowo AR, Bae DM, Sohn JM, Zakki AF, Cao B, Cho JH. Effects of the rebounding of a striking ship on structural crashworthiness during ship-ship collision. Thin-Walled Struct. 2017;115:225–39. doi: 10.1016/j.tws.2017.02.022.

[23] Zhang M, Zhu Z, Zeng Y, Liu J, Hu Z. Analytical method for evaluating the impact response of stiffeners in a ship side shell subjected to bulbous bow collision. Math Probl Eng. 2020;2020:5025438. doi: 10.1155/2020/5025438.

[24] Silveira P, Teixeira AP, Figueira JR, Soares CG. A multicriteria outranking approach for ship collision risk assessment. Reliab Eng Syst Saf. 2021;214:107789. doi: 10.1016/j.ress.2021.107789.

[25] Calle MAG, Oshiro RE, Alves M. Ship collision and grounding: scaled experiments and numerical analysis. Int J Impact Eng. 2017;103:195–210. doi: 10.1016/j.ijimpeng.2017.01.021.
[26] Rigueiro C, Ribeiro J, Santiago A. Numerical assessment of the behaviour of fixed offshore platform subjected to ship collision. Proc Eng. 2017;199:2494–9. doi: 10.1016/j.proeng.2017.09.415.
[27] Zhu L, Liu W, Fang H, Chen J, Zhuang Y, Han J. Design and simulation of innovative foam-filled Lattice composite bumper system for bridge protection in ship collisions. Compos B Eng. 2019;157:24–35. doi: 10.1016/j.compositesb.2018.08.067.
[28] Alsos HS, Amdahl J. On the resistance to penetration of stiffened plates, part I – experiments. Int J Impact Eng. 2008;36:799–807. doi: 10.1016/j.ijimpeng.2008.10.005.
[29] Salomon A. An evaluation of finite element models of stiffened plates. United States: Massachusetts Institute of Technology; 2001.